Morphological Characterization of Wax and Surfactant–Encapsulated Microcrystalline Cellulose for Better Dispersion

Qingzheng Cheng
Chengfeng Zhou
Yuanfeng Pan
Brian Via

Abstract

Encapsulation of cellulose with wax and surfactant is a physical way to restrict cellulose-to-cellulose attraction. Because wax is often used in the wood composite process, industrial manufacturers would not have to upgrade or add expensive equipment to handle cellulose addition. The encapsulated cellulose particles could easily be transported to composite and polymer facilities and blended in a homogeneous fashion for a multitude of products and composites. It was the objective of this study to utilize differential interference contrast (DIC) microscopy to characterize the wax and surfactant coverage and encapsulation morphology of the wax–surfactant–cellulose composite. The lengths and widths of the cellulose particles were significantly changed after encapsulation. DIC microscopy found that we could fine-tune wax coverage to control homogeneity and reduce fiber bundling during dispersion. It was found that surfactants were not necessary to enhance coverage if a 1:4 ratio of wax to microcrystalline cellulose was used. However, if more wax is desired, then surfactants may be necessary to suppress fiber bundles during dispersion.

Cellulose-based materials are becoming more of a value-added commodity and can be extracted from any plant material across the globe. Unlike lignin, cellulose is consistent within and between plant tissue types because of its linear and repeatable β(1→4)-linked D-glucose unit chain. Such a uniform material from a biological material makes cellulose unique compared with lignin, which is a complex three-dimensional polymer made up of p-hydroxyphenyl (H), guaiacyl (G), and syringyl (S) phenylpropanoid units that vary in polymerization, concentration, and distribution across plants (Ghaffar and Fan 2013). The cellulose microfibers are protected by a lignin sheath where the cellulose dictates stiffness while the lignin provides plastic deformation, particularly at high microfibril angles (Via et al. 2009). Other plants, such as flax, exhibit a complex relationship between pectic acid and microfibril angle to yield a negative correlation to tissue rupture (Via et al. 2009, Bourmaud et al. 2013). Although the lignin sheath provides additional matrix hardening and degradation resistance to fungi, its removal during industrial processing is more tedious and requires higher temperatures and solvent extraction. Thus, the thermochemical process necessary to yield pure cellulose is costly, so it is important to find profitable value-added uses for cellulose-based bioproducts for which cost is not prohibitive.

Cellulose is receiving increased attention for dispersion into various forest and paper products, wood composites, films, and wood plastic composites (Kojima et al. 2018, Murayama et al. 2018, Solikhin et al. 2018, Iglesias et al. 2020). Cellulose fibers are becoming a more viable option

The authors are, respectively, Research Fellow, Forest Products Development Center, School of Forestry and Wildlife Sci., Auburn Univ., Alabama (qcheng@yahoo.com [corresponding author]); Lecturer, Lab. of New Fiber Materials and Modern Textile, State Key Lab. of Bio-Fibers and Eco-Textiles, Qingdao Univ., China, and Visiting Scholar, Forest Products Development Center, School of Forestry and Wildlife Sci., Auburn Univ., Alabama (Chengfengzhou828@gmail.com); Lecturer, School of Food Sci. and Pharmaceutical Engineering, Zaozhuang Univ., China, and Visiting Scholar, Forest Products Development Center, School of Forestry and Wildlife Sci., Auburn Univ., Alabama (ypan@uzz.edu.cn); and Professor and Director, Forest Products Development Center, School of Forestry and Wildlife Sci., Auburn Univ., Alabama (bkv0003@auburn.edu). This paper was received for publication in December 2019. Article no. 19-00070.

Forest Prod. J. 70(2):226–231.
doi:10.13073/FPJ-D-19-00070

for polymer and wood composites. The modulus of the fiber can be as high as 100 to 130 GPa when measured at the nanoscale and 40 GPa when tested in films (Cheng and Wang 2008, Dai et al. 2013, Dufresne 2013). Cellulose can be processed to microcrystalline or nanoscale size and be placed in various polymer and wood composites. Poly(vinyl alcohol) was reinforced with ultrasonically treated cellulose to make biodegradable nanocomposites through film casting (Cheng et al. 2009). Others placed cellulose and nanocellulose into phenol-formaldehyde (Veigel et al. 2012) and wood-based composites (Arta-Obeng et al. 2012) with significant gains in modulus. However, when larger microcrystalline cellulose was placed in particleboard, gains in modulus were not observed. In fact, the addition of cellulose resulted in a reduction in modulus. It was postulated that the rupture at the cellulose–adhesive interface was due to differences in springback between cellulose, wood, and the adhesive matrix on press release (Arta-Obeng et al. 2012). It was also seen that cellulose dispersion during blending was difficult because of cellulose-to-cellulose affinity. Modification for better hydrophobicity has been a common method to assist in dispersion (Missoum et al. 2013), but other ways could also be helpful.

Encapsulation of cellulose with wax is a physical way to restrict cellulose-to-cellulose attraction (Pan et al. 2014). Because wax is often used in the wood composite process at around 1 percent (wt/wt) loadings, industrial manufacturers would not have to upgrade or add expensive equipment to handle cellulose addition. The encapsulated cellulose particles could easily be transported to composite and polymer facilities and blended in a homogeneous fashion for a multitude of products and composites. However, because wax coverage would restrict bonding between the cellulose and polymer or adhesive, thin layers that can melt and flow during processing may be important. Incomplete coverage may also be beneficial in that the encapsulated portion of cellulose would provide a bulking effect and make it difficult for groups of cellulose fibers to agglomerate. Yet the exposed portion of cellulose could be available for bonding to the polymer or adhesive matrix and used for polymer reinforcement (Pan et al. 2016a, 2016b). Ways to microscopically characterize such coverage and morphology are important steps toward the development and application of encapsulated cellulose.

Differential interference contrast (DIC) microscopy has been available for some time, but recent improvements in performance and cost make it a new analytical tool for the characterization of cellulose-based fibers (Peter et al. 2003). DIC utilizes polarized light beams that concurrently illuminate a thin tissue or particle with two perpendicular light beams, resulting in a three-dimensional appearance on a two-dimensional plane (Rojas et al. 2009). Visually, there is a shadow effect in which the topography of the cellulose particle can be enhanced through shadow contrasting. This allows for better estimation of wax coverage during cellulose encapsulation, while general image analysis tools can be employed to understand the shape morphology of the cellulose–wax composite. Compared with scanning electron microscopy (SEM) and atomic force microscopy, the advantages of DIC microscopy include easier operation, lower cost, and that it can be used for larger samples (up to hundreds of microns) and is suitable for wax–microcrystalline cellulose (MCC) encapsulation characterization.

The objective of this article was to utilize DIC microscopy to characterize the wax encapsulation morphology of the wax–cellulose composite. A new encapsulation method was demonstrated that is simple and cheap for industrial processing (Pan et al. 2014, 2016a, 2016b). Relationships between recipe formulation and morphology will be explored to determine the different recipes that would be necessary to achieve a given morphology. This work can help yield optimal recipes for a desired coverage and encapsulation shape of wax–cellulose composites that incorporate wax-covered cellulose into polymer- and wood-based composites.

Materials and Methods

Materials

Paraffin wax was purchased from Gulf Oil Corporation (USA). Two surfactants (Span 60 and Tween 40) were purchased from VWR Chemical Company (USA). MCC was purchased from VWR Chemical and has an average diameter of 90 μm.

Cellulose capsulation

The cellulose particles were capsulated with wax and mixtures of surfactants and wax, respectively, in this study. The components of the three encapsulated cellulose with wax and mixtures of surfactants and wax are shown in Table 1. The ratio of the two surfactants (span:Tween = 7:3) was chosen because it was the best ratio to make small wax spheres in order to improve cellulose capsulation, since smaller wax spheres can make thinner layers on the cellulose surfaces, and the ratio of surfactants and wax of 1:20 was used for the mixture (Pan et al. 2014). The process to capsulate the MCC particles using wax and mixtures was a modified microcapsule synthesis method (Pan et al. 2014). Briefly, the wax and mixtures were mixed with the MCC particles while maintaining the temperature at 70°C with continuous mechanical stirring. The wax or mixtures were placed in a beaker and then stirred at 1,000 rpm for 5 minutes and melted completely at 70°C. Then cellulose particles were added with different ratios (Table 1) to the above mixtures with stirring at 1,000 rpm for 10 minutes. Finally, the temperature was decreased to room temperature with stirring at 300 rpm.

Morphology measurement and data analysis

All the final products were observed by an optical microscope (BX 53; Olympus, USA) under regular light mode and DIC mode. The Olympus BX53 provides advanced modularity to suit a variety of observation styles, such as bright field, phase contrast, fluorescence, DIC, and polarized light, and features four objectives: ×4, ×10, ×40, and ×100. SEM (EVO 50VP; Zeiss, Germany) was also used to confirm the images obtained by DIC. ImageJ software (National Institutes of Health 2019) was used to measure the length and width of the uncoated MCC and encapsulated MCC particles. One hundred particles were selected and measured from each group. The particles were from hundreds of images that were similar, as shown in Figure 1. The coverage of wax or wax and surfactant (WS)

Table 1.—Components of the three encapsulated cellulose with wax and mixtures of surfactants and wax.

Components[a]	Group A	Group B	Group C
W:MCC (W:M)	1:2	1:3	1:4
WS:MCC (WS:M)	1:2	1:3	1:4

[a] MCC = microcrystalline cellulose; W = wax; WS = wax and surfactant.

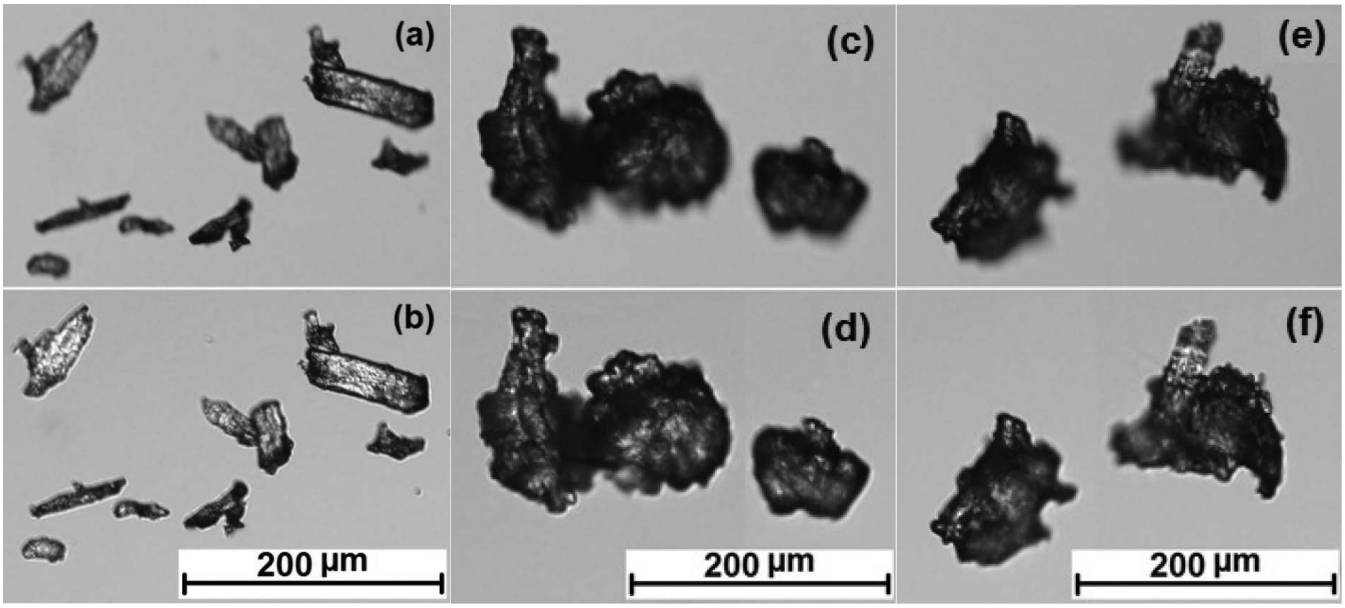

Figure 1.—Images of uncoated microcrystalline cellulose (MCC) (a, b), wax-coated MCC (c, d), and wax and surfactant–coated MCC (e, f) from regular light microscopy (a, c, and e) and differential interference contrast light microscopy (b, d, and f).

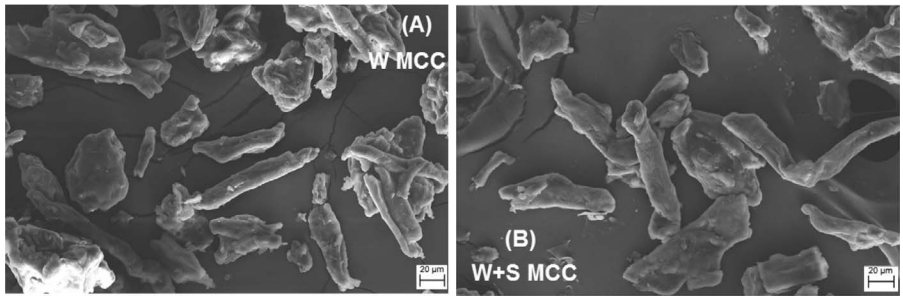

Figure 2.—Scanning electron microscopy images of (A) wax (W)-coated microcrystalline cellulose (MCC) and (B) wax and surfactant (WS)–coated MCC.

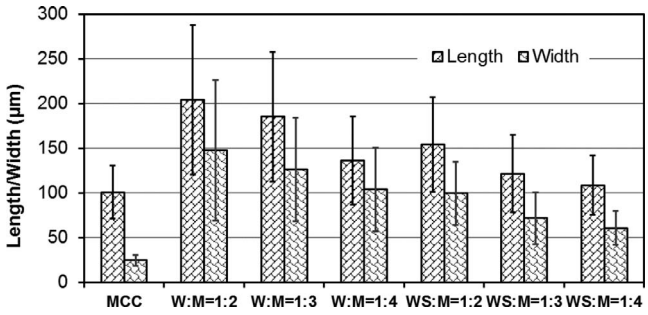

Figure 3.—Changes of lengths and widths of microcrystalline cellulose (MCC) particles before and after coating with wax (W) and wax and surfactant (WS).

mixtures was observed from the DIC images and divided into four groups: nonencapsulated (no coating materials on single MCC particles), partly encapsulated (only part of the single MCC particles covered by coating materials), fully encapsulated (single MCC particles wholly covered by coating materials), and bundle encapsulated (two or more MCC particles partly or wholly covered by coating materials). The coverage percentages of the untreated MCC and encapsulated MCC particles were calculated and compared. Analysis of variance ($\alpha = 0.05$) was used to examine differences between the samples (t tests).

Results and Discussion

Image comparisons using DIC, regular light microscopy, and SEM

Figure 1 shows images of uncoated MCC, wax-coated MCC, and WS-coated MCC from regular light microscopy (a, c, and e) and DIC light microscopy (b, d, and f), provided that DIC images had better visible features than those from light microscopy. Figure 2 shows SEM images of wax-coated MCC and WS-coated MCC, which showed the differences in wax coverage and particle size and indicated that wax-coated MCC (Fig. 2A) had more particle bundles than WS-coated MCC (Fig. 2B).

MCC length and width changes after coating with wax and WS

Figure 3 shows the length and width changes of MCC particles after coating with wax and WS. All the lengths of coated MCC were significantly longer than those of uncoated MCC ($P < 0.05$), except WS:M = 1:4, which

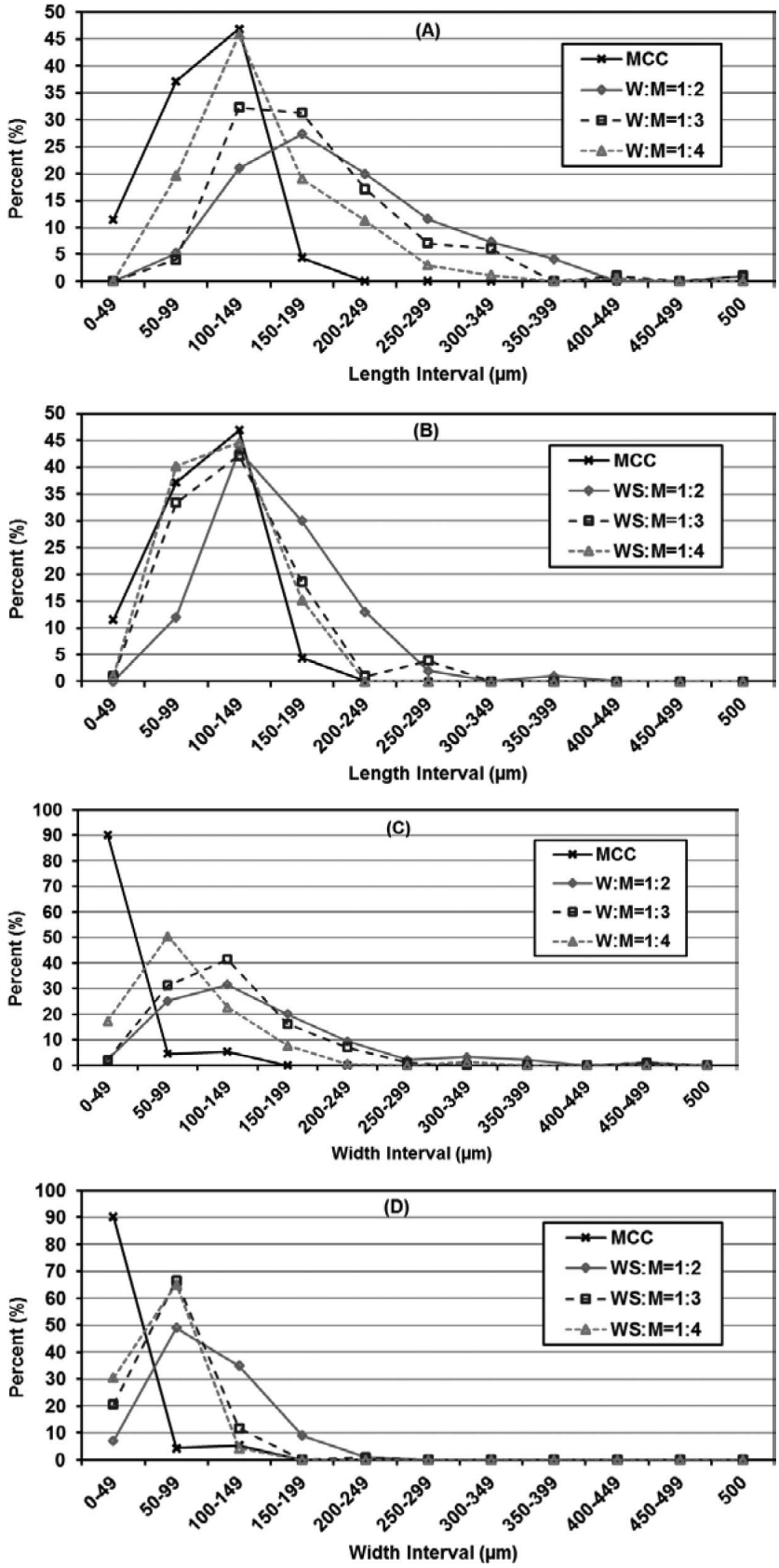

Figure 4.—Length and width distributions of microcrystalline cellulose (MCC) particles before and after coating with wax (W) and wax and surfactant (WS).

has a P value of 0.046. This difference indicated that the coatings extended the MCC particles and/or that the coated MCC particles were MCC bundles, as shown in Figures 1 and 2. Similar to the lengths, the widths of coated MCC were significantly larger than those of uncoated MCC ($P < 0.05$). For both wax-coated and WS-coated MCC particles, the lengths and widths were nearing the uncoated MCC lengths and widths along with the wax and WS loading decreasing, respectively. WS-coated MCC particles had lower lengths and widths compared with those of the wax-coated MCC with corresponding wax or WS ratios, which indicated that the surfactant helped the wax disperse on the MCC surfaces, and WS-coated MCC (Fig. 2B) had fewer bundles than wax-coated MCC (Fig. 2A; Pan et al. 2014). Therefore, the lengths and widths of the particles were significantly changed after encapsulation due to the wax or the mixture covered on the particle surfaces and particle bundles.

Length and width distributions of wax-coated and WS-coated MCC particles

The length (Figs. 4A and 4B) and width (Figs. 4C and 4D) distributions of MCC particles before and after coating with wax and WS are shown in Figure 4. All the lengths of coated MCC were significantly longer than those of uncoated MCC. The more wax (Fig. 4A) or WS (Fig. 4B) was used, the longer the particles/bundles obtained, and the median values (100 to 149) were closer to those of uncoated MCC. However, the length distribution of WS-coated particles had smaller median length values and narrower ranges (Fig. 4B) compared with those of wax-coated MCC (Fig. 4A). This illustrates again that the surfactant helped the wax disperse on the MCC surfaces and WS-coated MCC since surfactant makes smaller wax spheres, which can make thinner layers on the cellulose surfaces and improve cellulose capsulation. The width distributions of coated MCC (Figs. 4C and 4D) had similar changing trends to the length distributions, and WS-coated MCC particles had smaller median width values and narrower ranges (Fig. 4D) compared with those of wax-coated MCC (Fig. 4C).

Coverages of wax and WS on MCC particles

Figure 5 shows the coverages of wax (Fig. 5A) and WS (Fig. 5B) on the coated MCC particles. When more wax was used (W:M or WS:M = 1:2), there were fewer nonencapsulated and more bundle-encapsulated MCC particles. When less wax was used (W:M or WS:M = 1:4), there were more nonencapsulated MCC particles and many more fully-encapsulated, but fewer bundle-encapsulated particles, which could be a benefit for the particle dispersion in the composite materials. According to these ratios and MCC and wax additions to the designed composites, an optimized W:M or WS ratio can be calculated before the encapsulated MCC particles are made.

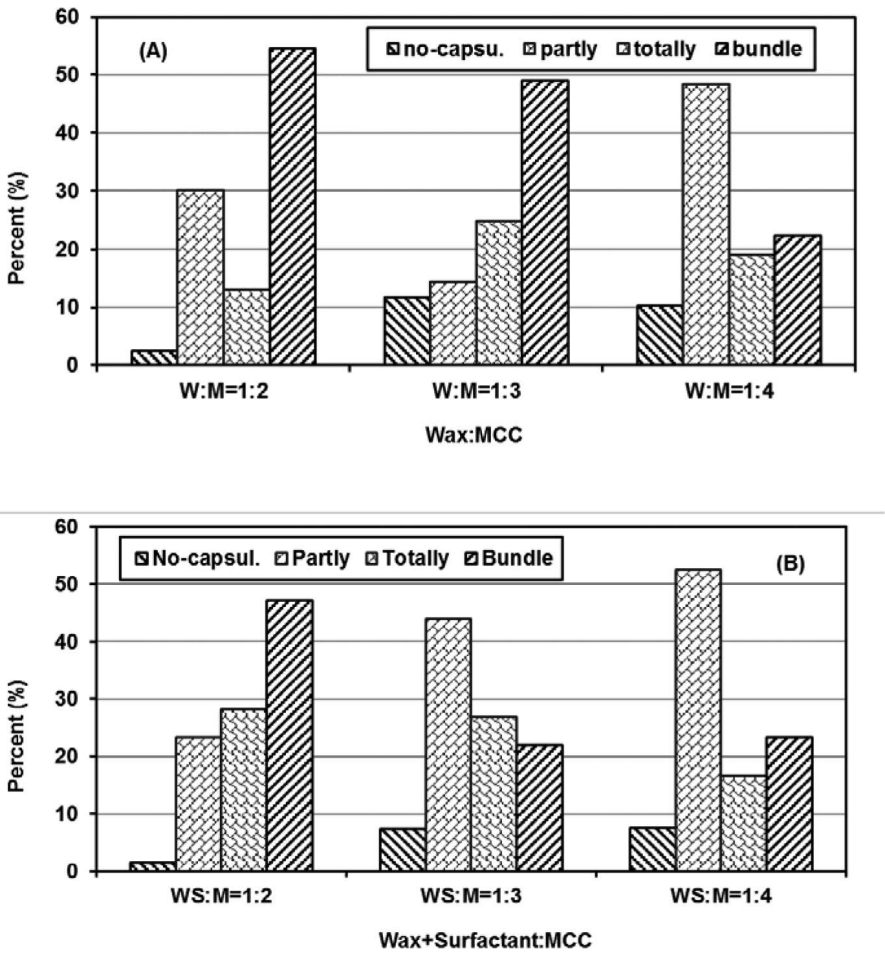

Figure 5.—Coverages of (A) wax (W) and (B) wax and surfactant (WS) on microcrystalline cellulose (MCC) particles.

Conclusions

MCC particles can be successfully encapsulated with paraffin wax and mixtures of wax and surfactant. Surfactants are helpful for the dispersion of the wax on the surfaces of MCC particles. DIC microscopy is better than regular microscopy to characterize the coverage and encapsulation morphology of the MCC particles coated with wax and the mixtures of wax and surfactant. The lengths and widths of the particles were significantly changed after encapsulation. The coverages with wax and the mixtures of wax and surfactant were also changed with the changing ratios of wax or the mixtures of wax and surfactant to MCC. When less wax was used, there were more nonencapsulated and many more fully-encapsulated particles, but fewer bundle-encapsulated particles, which could be a benefit for the particle dispersion in the composite materials. An optimized ratio of wax to MCC or WS to MCC can be calculated according these ratios and MCC and wax additions to the designed composites because wax is often used in the wood composite process. The encapsulated cellulose particles could easily be transported to composite and polymer facilities and blended in a homogeneous fashion for a multitude of products and composites.

Acknowledgments

The authors gratefully acknowledge financial support by the State Key Laboratory of Bio-Fibers and Eco-Textiles (KFKT04), Regions Bank, and the China Scholarship Council. The authors appreciate the support from colleagues and graduate students in the Forest Products Development Center, Auburn University.

Literature Cited

Arta-Obeng, E., B. K. Via, and O. Fasina. 2012. Effect of microcrystalline cellulose, species, and particle size on mechanical and physical properties of particleboard. *Wood Fiber Sci*. 44:227–235.

Bourmaud, A., C. Morvan, A. Bouali, V. Placet, P. Perre, and C. Baley. 2013. Relationships between micro-fibrillar angle, mechanical properties and biochemical composition of flax fibers. *Ind. Crops Prod*. 44:343–351.

Cheng, Q. and S. Wang. 2008. A method for testing the elastic modulus of single cellulose fibrils via atomic force microscopy. *Compos. Part A Appl. Sci. Manuf*. 39:1838–1843.

Cheng, Q., S. Wang, and T. G. Rials. 2009. Poly(vinyl alcohol) nanocomposites reinforced with cellulose fibrils isolated by high intensity ultrasonication. *Compos. Part A Appl. Sci. Manuf*. 40:218–224.

Dai, D. S., M. Z. Fan, and P. Collins. 2013. Fabrication of nanocelluloses from hemp fibers and their application for the reinforcement of hemp fibers. *Ind. Crops Prod*. 44:192–199.

Dufresne, A. 2013. Nanocellulose: A new ageless bionanomaterial. *Mater. Today* 16:220–227.

Ghaffar, S. H. and M. Z. Fan. 2013. Structural analysis for lignin characteristics in biomass straw. *Biomass Bioenergy* 57:264–279.

Iglesias, M. C., D. Gomez-Maldonado, B. K. Via, Z. Jiang, and M. S. Peresin. 2020. Pulping processes and their effects on cellulose fibers and nanofibrillated cellulose properties: A review. *Forest Prod. J*. 70(1):10–21.

Kojima, Y., N. Kato, K. Ota, H. Kobori, S. Suzuki, K. Aoki, and H. Ito. 2018. Cellulose nanofiber as complete natural binder for particleboard. *Forest Prod. J*. 68(3):203–210.

Missoum, K., F. Martoia, M. N. Belgacem, and J. Bras. 2013. Effect of chemically modified nanofibrillated cellulose addition on the properties of fiber-based materials. *Ind. Crops Prod*. 48:98–105.

Murayama, K., M. Yamamoto, H. Kobori, Y. Kojima, S. Suzuki, K. Aoki, H. Ito, S. Ogoe, and M. Okamoto. 2018. Mechanical and physical properties of wood–plastic composites containing cellulose nanofibers added to wood flour. *Forest Prod. J*. 68(4):398–404.

National Institutes of Health. 2019. ImageJ. http://imagej.nih.gov/ij. Accessed March 1, 2019.

Pan, Y., Y. Liu, Q. Cheng, Y. Celikbag, B. K. Via, X. Wang, and R. Sun. 2016a. Surface coating of microcrystalline cellulose with surfactants and paraffin wax. *Eur. J. Wood Wood Prod*. 74:763–765. DOI:10.1007/s00107-016-1030-5

Pan, Y., Y. Pan, Q. Cheng, Y. Liu, C. Essien, B. K. Via, X. Wang, R. Sun, and S. Taylor. 2016b. Characterization of epoxy composites reinforced with wax encapsulated microcrystalline cellulose. *Polymers* 8(12):415. DOI:10.3390/polym8120415

Pan, Y., S. Sun, Q. Cheng, Y. Celikbag, B. Via, X. Wang, and R. Sun. 2014. Technical note: Melt dispersion technique for preparing paraffin wax microspheres for cellulose encapsulation. *Wood Fiber Sci*. 46(4):1–6.

Peter, G. F., D. M. Benton, and K. Bennett. 2003. A simple, direct method for measurement of microfibril angle in single fibres using differential interference contrast microscopy. *J. Pulp Paper Sci*. 29:274–280.

Rojas, J. A. M., J. Alpuente, I. M. Rojas, and S. Vignote. 2009. Fractal-based image enhancement techniques inspired by differential interference contrast microscopy. *J. Optics Part A Pure Appl. Optics* 11(6):065503.

Solikhin, A., Y. S. Hadi, M. Y. Massijaya, S. Nikmatin, S. Suzuki, Y. Kojima, and H. Kobori. 2018. Reinforcement effects of microfibrillated cellulose on chitosan–polyvinyl alcohol nanocomposite film properties. *Forest Prod. J*. 68(3):216–225.

Veigel, S., J. Rathke, M. Weigl, and W. Gindl-Altmutter. 2012. Particle board and oriented strand board prepared with nanocellulose-reinforced adhesive. *J. Nanomater*. 2012:158503.

Via, B., C. So, T. Shupe, L. Groom, and J. Wikaira. 2009. Mechanical response of longleaf pine to variation in microfibril angle, chemistry associated wavelengths, density, and radial position. *Compos. Part A Appl. Sci. Manuf*. 40:60–66.